Comparison of Sound-Source Localization Techniques for Vibrating Structures

M. Müller-Trapet [1], P. Dietrich[1]

[1] *Institute of Technical Acoustics, RWTH Aachen University, Email: mmt/pdi@akustik.rwth-aachen.de*

Introduction

Besides the well established non-contact sound-source localization methods – laser vibrometry and intensity measurements – the beamforming technique has become very popular in the last decade and several commercial products are already available [1, 2, 3]. Although extensive research has been carried out in the last years, investigations have been either purely theoretical, making theoretic assumptions on the source and the sound radiation, or measurements were conducted in the field, not allowing the source properties and imperfections of the measurement equipment to be controlled. Hence the question how the theoretical observations correspond to real situations.

The approach that will be presented in this paper can be used to investigate the performance of beamforming under realistic conditions. First, real input data is obtained by measuring the velocity distribution on the test object. This data is used to simulate the sound radiation with the Boundary Element Method (BEM). This procedure allows the calculation of the beamforming output for any array geometry avoiding the problems of microphone imperfections or signal acquisition. Furthermore, the beamforming results can directly be compared to the simulated sound intensity, as shown in Figure 1.

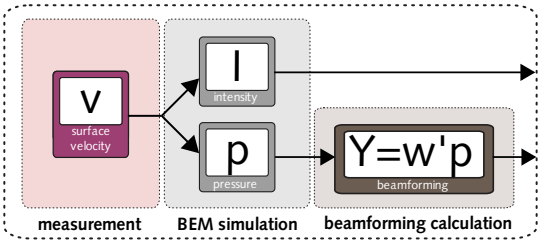

Figure 1: Schematic of the presented approach

As a practical example, metal plates and wooden boards were excited with a mechanical shaker and scanned with a Laser Doppler Vibrometer. The sound radiation towards the microphones of different array geometries was simulated and the beamforming output was calculated for the Delay-and-Sum algorithm and finally compared to the sound intensity. In this paper, results will be presented for a metal plate of 1 mm thickness.

Surface Velocity Measurements

To obtain real input data for the BEM simulations the surface velocity was measured with the Laser Vibrometer on four different plates. The measurement setup is shown in Figure 2. In total, two metal plates and two wooden

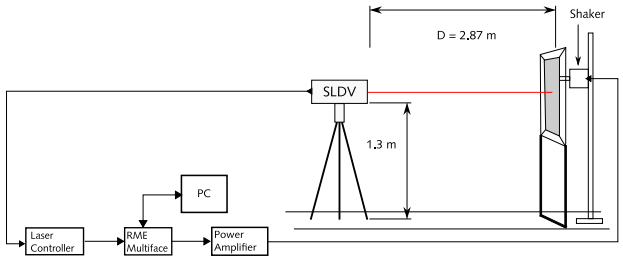

Figure 2: Schematic of the measurement setup for the velocity measurements

boards were excited by a mechanical shaker at three different points (Figure 3) and the impulse responses were measured succesively at a regular grid on the plate. The scan grid consisted of 5041 points spaced 0.01 m to avoid spatial aliasing, accounting for the different relation between wavelength and frequency for bending waves on plates. With this setup, the velocity distribution in the frequency range between 200 Hz and 10 kHz was determined and used as input for the BEM simulations.

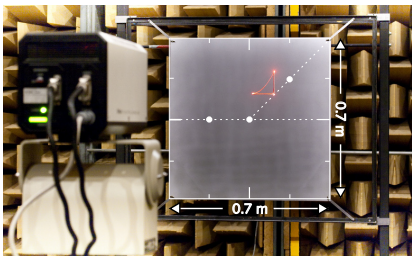

Figure 3: Measurement setup of the velocity measurements, with excitation points marked by white circles

BEM Simulations

The sound radiation from the plates was simulated numerically with the Boundary Element Method (BEM) using LMS VirtualLab/Sysnoise as a solver. In order to fulfill the six-element-per-wavelength requirement, the measured velocity data had to be interpolated to a finer grid that had twice as many points per dimension, which resulted in a mesh of 19881 nodes, spaced at 0.005 m. The sound radiation was then calculated at the $^1/_{24\text{th}}$ octave-band center frequencies between 200 Hz and 10 kHz in a two step process: in the first step, the pressure directly in front of the plate surface resulting from the given boundary conditions was determined and in the second step the radiation towards the field points was calculated. In this case, the field points represent the array microphones.

The setup for the BEM simulations is presented in

Figure 4. In total, six different array geometries with 32 microphones at two meters distance from the plates were simulated. Additionally, the sound intensity was calculated in a plane 0.1 m in front of the plates.

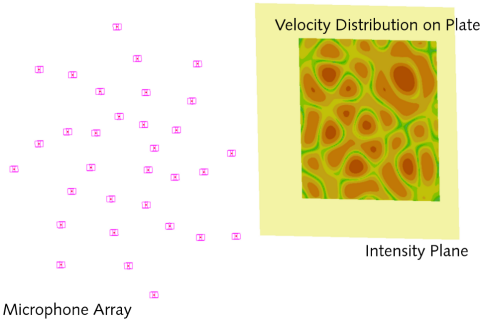

Figure 4: Simulation setup for the BEM simulations; the array is located at 2 m distance from the plate, the intensity was calculated in a plane 0.1 m in front of the plate

Beamforming Calculations

With the simulated sound pressure available at the array microphones, the squared beamforming output could be calculated according to the general frequency-domain beamforming equation, as defined, for example in [4]:

$$|Y|^2 = \mathbf{w}'\mathbf{R}\mathbf{w} \tag{1}$$

where $\mathbf{w}' \equiv (\mathbf{w}^*)^T$ is the complex conjugate transpose of the weight vector $\mathbf{w}$ and $\mathbf{R} = \mathbf{p}\mathbf{p}'$ is the cross spectral matrix, with $\mathbf{p}$ as the vector of pressures at the microphones. The weight vector for the Delay-and-Sum beamformer, which was used for the results presented in this paper, is the normalized steering vector $\mathbf{w} = \frac{1}{M}\mathbf{v}$, where M is the number of microphones and $\mathbf{v}$ is the steering vector.

The squared beamforming output was calculated at the frequencies from the BEM simulations and then averaged per third-octave band for the evaluation. The scanning plane was equal to the plane where the sound intensity was calculated.

Results

The results in this paper are presented for a metal plate of 1 mm thickness excited at the left position (Figure 3). A logarithmic spiral array with 32 microphones was chosen as the setup, as this is the geometry with the best performance and hence one of the most commonly used array types.

Sound Power The sound power was calculated by integrating the intensity and the squared beamforming output, divided by $Z_0 = \rho_0 c = 414\,\mathrm{kg/m^2 s}$, over the surface of the intensity plane and the scanning plane, respectively. As can be seen from Figure 5, the sound power from the beamforming result (green curve) shows a dependency on frequency, which can be related to the Half-Power Beam Width (HPBW) [2], so that for low frequencies the beamformer overestimates the pressure. Due to this fact, the results of the beamformer had to be adjusted in order to compare the source maps to the sound intensity; the red curve shows the sound power of the beamformer with the level adjustment.

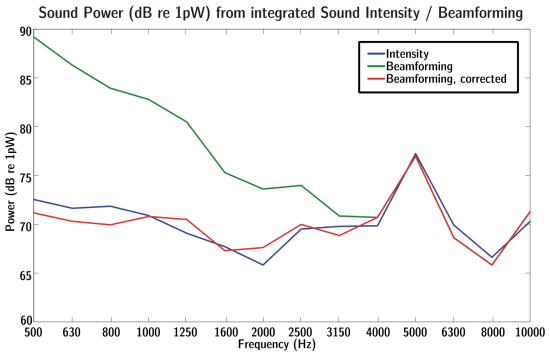

Figure 5: Source Power, calculated by integrating the simulated Intensity (blue) and the beamforming output from the simulated pressure at the array microphones (green and red)

A single adjustment factor for the entire beamforming source map cannot be exact, since the beam width is not only dependent on frequency, but also on the array geometry and the steering direction, as shown in Figure 6, where the beampattern for the logarithmic spiral array at 1 kHz is plotted for the broadside direction and for the steering direction 30° away from broadside. It can be observed how the beam widens as it is steered away from broadside. This suggests, that any adjustment has to take the steering direction and the array geometry into account.

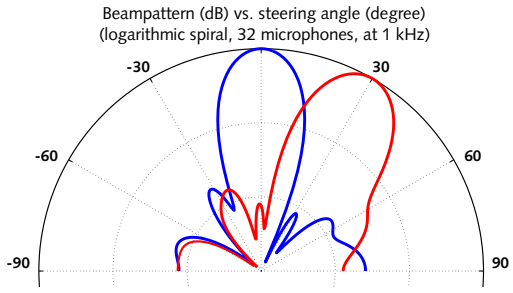

Figure 6: Beampattern for the logarithmic spiral array with 32 microphones at 1 kHz: blue – steered at broadside, red – 30° from broadside

The correction applied here was, however, not intended to achieve an exact source power but just as an equalization factor with the goal of comparing the source maps to the sound intensity, so it was sufficient to use an approximate factor.

Beamforming vs. Intensity With the adjusted power level, the beamforming source maps from the simulated sound pressure at the array microphones could now be compared to the simulated sound intensity (Figure 7 and Figure 8, for the 2 kHz third-octave band and the 4 kHz third-octave band, respectively). Clearly, the source distribution can be approximated very well

from the beamformer, with the wider beamwidth at lower frequencies as a restriction on the spatial resolution. In general, there is a high similarity between the intensity and the beamforming source maps for all the plates that were tested and for the entire frequency range.

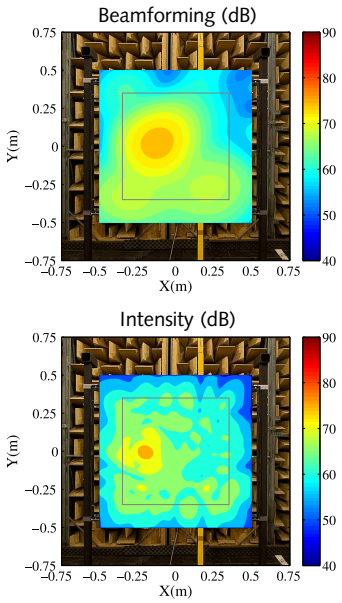

Figure 7: Beamforming source map from the simulated pressure at the array microphones (top) vs. simulated Intensity (bottom) for the 2 kHz third-octave band

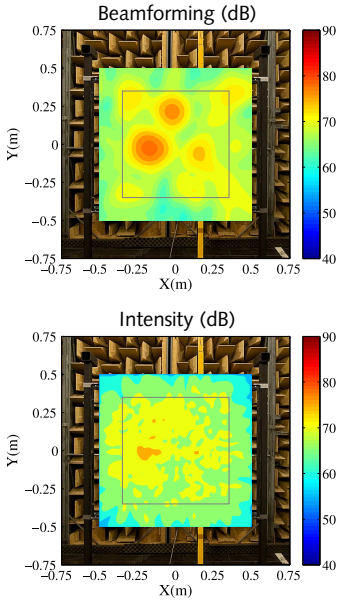

Figure 8: Beamforming source map from the simulated pressure at the array microphones (top) vs. simulated Intensity (bottom) for the 4 kHz third-octave band

Comparative measurements

In order to validate the presented approach, measurements of a real array setup with the metal plate as the test object were performed in the semi-anechoic chamber of the institute. For this purpose, a lightweight, variable array support made of aluminum pipes of small diameter (Figure 9) was built, which allows the setup of the most common planar array geometries with up to 64 microphones, with the only restriction of a maximum diameter of 1.5 m.

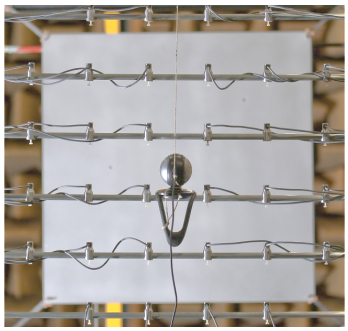

Figure 9: Setup with the array support in the semi-anechoic chamber, all parameters and dimensions are the same as in the BEM simulations

In this respect, the advantage of the simulation setup played a major role because of the ability to simulate the complete array setup to investigate the effects of reflection and diffraction on the result. This provided a realistic estimate of what could be expected from the measurement results.

For the beamforming measurements, the plate was excited again with the mechanical shaker, only that now the signal was broadband white noise. The array geometry used for the measurements was a regular grid with 0.1 m inter-element spacing, which had also been simulated before. The results of the beamforming output for the measured microphone pressures in comparison with the simulated results (for the same array) are presented in Figure 10 and Figure 11.

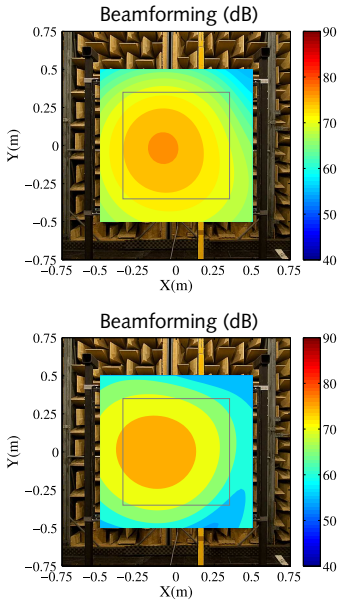

Figure 10: Beamforming source map from the simulated pressure (top) vs. beamforming source map from the measured pressure (bottom) for the 2 kHz third-octave band

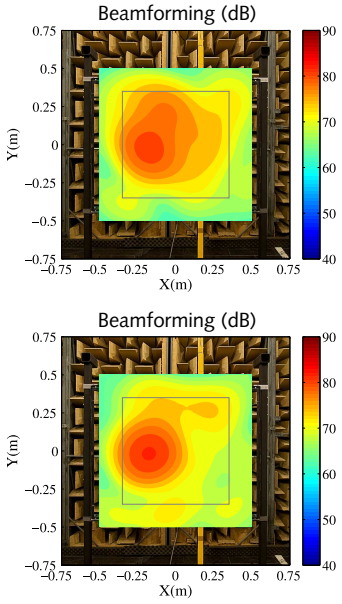

Figure 11: Beamforming source map from the simulated pressure (top) vs. beamforming source map from the measured pressure (bottom) for the 4 kHz third-octave band

The measurements agree very well with the simulations, keeping in mind that the results were also corrected as before in order to be comparable. Slight deviations of the measured source maps can be explained from the difficult measurement conditions: the floor between the plate and the array was reflective and a certain amount of energy was also introduced into the stand, that the plate was mounted on, and then radiated from its edges. The sound radiated from the shaker itself also had a significant effect. In order to achieve a better result, foam pads were attached to the stand and placed on the floor in front of the array. Although this improved the result, not all reflections and unwanted radiation could be avoided.

For further measurements, a better separation between the excited plate and the structure it is mounted on has to be found, because the microphone array will always detect the radiation from both the plate and the surroundings, which is not covered by the simulation, as only the surface velocity on the plate is known.

Conclusion and Outlook

It was confirmed in this paper that the approach of calculating beamforming results from simulated radiation with real velocity input data is valid. This setup can now be used for further research, investigating the effect of

- different array geometries
- different algorithms – an adaptive algorithm according to *Capon* [5] and a deconvolution approach [6] have already been implemented
- variation of the Signal-to-Noise Ratio (SNR) at the array microphones
- array imperfections (uncertainties in the location, deviation from the exact geometry, deviation from the omni-directional directivity pattern of the microphones).

The results obtained after varying all these parameters can then be compared to the ideal result without any perturbations. Further measurements with real array setups will be performed and compared to the simulations.

It was also shown that a direct comparison of the beamforming results to the sound intensity is not possible due to the dependency of the power on the beam width for extended sources. The question of an appropriate scaling factor still remains. In [2], such a scaling factor is derived, but it will have to be verified.

A similar investigation has been carried out by Washburn et al. [7], where the sound power of heavy land-moving machinery was determined and compared to beamforming results. They use the scaling factor from [2], but find that the beamformer overestimates the power in the high frequency bands.

References

[1] S. Guidati and R. Sottek. Visualization of Sound Sources in Real Time: Microphone Array Processing Beyond the State of the Art. Noise-Con 2008 and the Sound Quality Symposium 2008.

[2] J. Hald. Combined NAH and Beamforming Using the Same Array. Brüel&Kjær Technical Review, 2005.

[3] Acoustic Camera. http://www.acoustic-camera.com

[4] D.H. Johnson and D.E. Dudgeon. Array Signal Processing: Concepts and Techniques. Prentice Hall, 1993.

[5] J. Capon. High-Resolution Frequency-Wavenumber Spectrum Analysis. Proceedings of the IEEE, 57(8):1408-1418, 1969.

[6] P. Sijtsma. CLEAN Based on Spatial Source Coherence. International Journal of Aeroacoustics, 6(4):357-374, 2007.

[7] K. Washburn et al. Correlating Noise Sources Identified By Beamforming With Sound Power Measurements. SAE International, 2005